Swumble™ In-Cylinder Fluid Motion for High Efficiency Gasoline SI Engines: development of the second generation

X. GAUTROT, M. BARDI, T. LEROY, P. LUCA, L. NOWAK, B. REVEILLE

IFP Energies nouvelles, 1 et 4 avenue de Bois-Préau, 92852 Rueil-Malmaison, France ; Institut Carnot IFPEN Transports Energie

Abstract: Global warming and air quality concerns, which are tackled thanks to ever more stringent emissions regulations, require to improve internal combustion engine efficiency and its emissions levels. Focusing on spark ignition engines, the main trend is to increase the compression ratio in combination with the use of Miller/Atkinson cycles. One well-known drawback of Miller/Atkinson cycles is the reduction of the in-cylinder fluid motion and thus a loss of turbulent kinetic energy, resulting in a decrease of the combustion speed thereby limiting the engine efficiency gains. To improve this, IFP Energies nouvelles (IFPEN) has developed a complex in-cylinder fluid motion: the so-called Swumble™.

The development of this innovative approach was achieved through the use of intensive 3D CFD calculations that showed a huge increase of the TKE produced when coupled to Miller / Atkinson cycles, without decreasing the flow capacity of the intake system. This allows the use of even more aggressive compression ratios and Miller cycles. In a second phase, single cylinder engine (SCE) tests confirmed the improved combustion speed. A greater capacity for dilution and an important reduction in engine out particles was also demonstrated. Finally, a brand new multi-cylinder engine (MCE) was designed, embedding this new generation of Swumble™ combustion system. Maximum power output of 90 kW/L was achieved with a brake efficiency higher than 41% on a significant area of the engine map.

Keywords: Spark Ignited engine, high efficiency, innovative fluid motion, Swumble™, Miller cycle

1 Introduction

The transport and mobility sector has for several years been facing major energy and environmental challenges imposing rapid and constant change. Reducing greenhouse gases (GHG) and air pollutant emissions is one of the major concerns of the transportation sector, driven by the evolutions of the different emissions regulations all over the world. The transport sector is responsible for 20 % of GHG emissions in Europe [1], and 25 % worldwide. Among these, road transportation represents the majority of the total GHG emissions, reaching 72 % in Europe [2], and 71 % worldwide (2018 [3]). It is estimated that in order to comply with the COP21 treaty objectives, CO_2 emissions should be further reduced by 50 to 85% from 2000 levels by year 2050 [4]. More specifically, the light-duty vehicle transportation target in Europe is to improve the overall GHG impact by approximately 60 % [1].

In this context, reducing the GHG emissions and the energy needs will require to act on various levels: powertrains and vehicle technologies, de-fossilisation of energy carriers, new mobility uses and services. Hybrid electric powertrains are considered as the primary mid-term solutions to lower fuel consumption and exhaust pollutant emissions, but in addition to hybridization, increasing internal combustion engine (ICE) efficiency is mandatory to reduce carbon dioxide (CO_2) emissions of the global fleet of vehicles. Moreover, minimization of CO_2 emissions is a prerequisite for ICE to remain a powertrain for future mobility. Figure 1 below illustrates what can be achieved in terms of CO_2 emissions reduction on the WLTC cycle when improving the efficiency of the ICE.

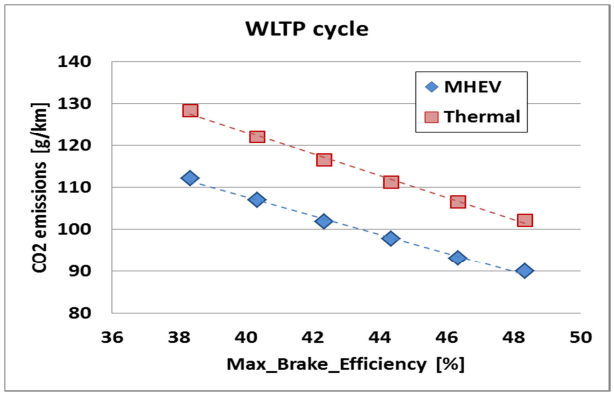

Figure 1. Impact of peak engine efficiency on CO_2 emissions of thermal and MHEV vehicles.

To respond to this concern, IFPEN developed the Swumble™ concept, an innovative approach for high efficiency combustion. Swumble™ enhances air turbulence, and is particularly well adapted to Miller strategies and high dilution rates, and thus improves

the engine efficiency over a large range of operating conditions. The works here presented will highlight the optimization tasks that have been performed, and the resulting outcomes that have been achieved on the final multi-cylinder engine.

2 3D CFD computations

2.1 Engine development

A spark ignited, tumble oriented, direct injection engine is used as base case for the Swumble™ development on both Miller and Atkinson cycles. The geometrical parameters are described in table 1.

Engine displacement		0.4 l
Volumetric compression ratio		13.0 : 1
Bore x Stroke (mm)		75 x 90.5
Number of intake / exhaust valves		2 / 2
Valve Lift duration, at 1mm (°CA)	Intake Miller / Atkinson	140 / 245
	Exhaust	210

Table 1. Single cylinder engine characteristics.

Masks are being used on the intake side of the combustion chamber for higher airflow velocities and better flow orientation at low lifts.

Simulation parameters: The boundary conditions are imposed at the cylinder head intake and exhaust ports entrances without the presence of plenums. This simplification was applied since pressure data coming from experimental measurements for both intake and exhaust sides was employed for the boundary conditions. All configurations computed during the Swumble™ development (Miller & Atkinson) share these boundary conditions. All RANS computations were executed using the CONVERGE™ software with default parameters for the solver. For the ignition, the ISSIM model [5] was used and for the combustion, the ECFM model [6] was employed. The objective is to assess the performances on both the aerodynamic and combustion phases on a second calculated engine cycle for better representation of the phenomenology. It should be noted that no injection was simulated and that a homogeneous mixture at stoichiometric ratio is imposed at the computational domain entrance.

Operating point: The development was focused on obtaining increased levels of efficiency and therefore an operating point of 12 bar IMEP and 2500 RPM was selected on the engine map for both Miller and Atkinson cycles for performance evaluations.

2.2 The Swumble™ concept

Existing optimisation strategies: It was previously proven in the work done by Cordier et al. [7] that when using Atkinson or Miller cycles (applying respectively later or earlier intake valve closing with respect to the bottom dead centre) a decrease in pumping work and heat losses is observed. The same work highlights the possibility to combine these strategies with higher compression ratios for further improvement in thermal efficiency while at the same time reducing the knock sensitivity towards high loads. However, combining these strategies comes with new challenges. By using the Miller cycle for example, high loss of aerodynamics and subsequent turbulence close to TDC was observed, which leads in the end to higher combustion duration and poor performances. [7]

Internal aerodynamic motion: It is well known that the motion inside the ICE is described with respect to the three axis of reference (X, Y, Z) illustrated in Figure 2.

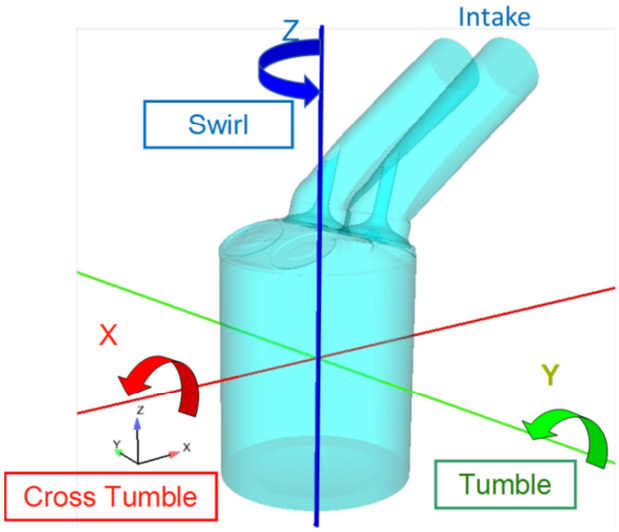

Figure 2. Different fluid motions in an internal combustion engine [8].

For better turbulence performance close to TDC, higher tumble levels have been targeted using different devices (flaps in the intake ports for example) [9-10]. The drawback of these kinds of approaches is that they tend to impede the flow capacity and therefore reduce the mass of fresh air admitted during the intake process. The Swumble™ concept, however, aims to obtain increased levels of turbulence close to TDC while using Atkinson / Miller cycles by combining all three motions. It consists in an innovative approach exclusively based on ducts and combustion chamber specific designs [8] without flow capacity degradation.

According to the CFD study done by Laget et al [11], increasing the in-cylinder charge motion improves the combustion phasing, MFB50 and its efficiency.

Nevertheless, since the turbulence intensity is increased, a reduction of the ignition delay, MFB10 is also observed. The ratio between tumble and swirl motions is a key parameter with regards to maximal heat release and maximum in-cylinder pressure. The tumble ratio component is dominant over the heat release, but according to Figure 3, the swirl motion reduces the knock sensitivity and therefore advances the combustion maximal in-cylinder pressure angle [12].

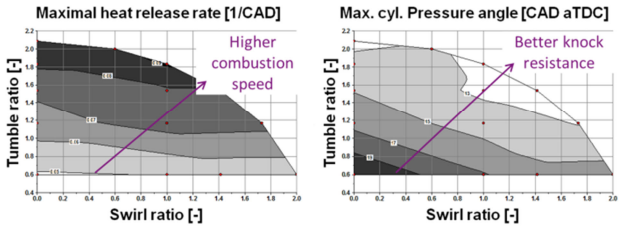

Figure 3. Maximal heat release and Maximal Pressure angle as a function of tumble and Swirl ratio [12].

All the above mentioned characteristics indicate that an optimised mix of tumble and swirl motions has the potential to improve the combustion efficiency. IFPEN has further improved its so called Swumble^{TM} engine taking advantage of all the latest knowledge and understandings.

2.3 Aerodynamic performances

The assessment of the engine aerodynamic performances (Miller and Atkinson cycles) is done on simulations which use identical numerical setups alongside with the same experimental data input. Geometrical differences are therefore the only source of any observed performance variations.

Trapped mass: Figure 4 indicates that when applying the Swumble^{TM} concept, the flow evolution is preserved without any important differences when compared to the base tumble oriented engine. The behaviour remains similar on both Miller and Atkinson cycles.

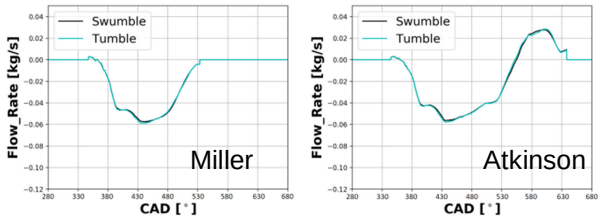

Figure 4. Flow rates comparison between Tumble and Swumble^{TM} engines for Miller and Atkinson cycles.

The Swumble^{TM} engine records a slight decrease of trapped mass (-0,7%) running on Miller cycle but 0,25% of gain running on the Atkinson cycle when compared to the Tumble base case.

Tumble:

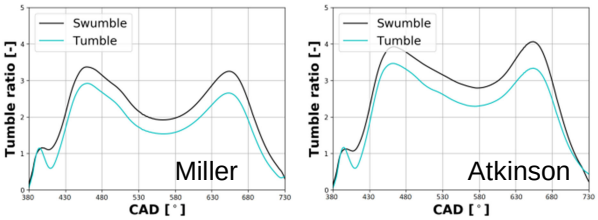

Figure 5. Tumble comparison between Tumble and Swumble^{TM} engines for Miller and Atkinson cycles

Looking at Figure 5, when using the Swumble^{TM} concept, a gain in tumble of 21% and 22% for Miller and Atkinson cycles respectively is observed at 70 CAD before the combustion TDC (720 CAD).

TKE (Turbulent Kinetic Energy):

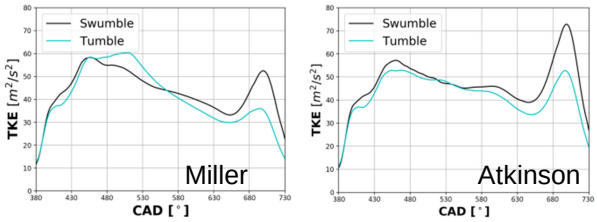

Figure 6. Turbulent Kinetic Energy comparison between Tumble and Swumble^{TM} engines for Miller and Atkinson cycles.

According to Figure 6, when using the Swumble^{TM} concept, a gain in TKE of 63% and 37% for Miller and Atkinson cycles respectively is observed at combustion TDC (720 CAD).

3D TKE post-processing:

The 3D post-processing consists of two views (refer to Figure 2 for reference planes): a vertical slice (parallel with XOZ) passing through the middle of the spark plug is shown on the upper half and on the lower half, a horizontal slice (parallel with XOY) at a height of 2 mm with respect to the piston head is displayed. The two planes are coloured by the TKE distribution. On both slices, the flame front is also represented as a solid black line.

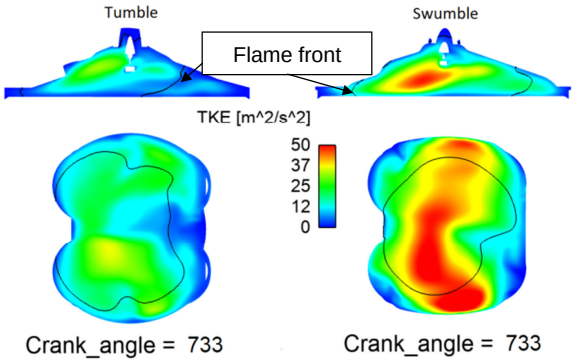

Figure 7. TKE distribution obtained and flame fronts on both Tumble and Swumble™ engines.

Figure 7 displays the comparison of the results obtained running on Miller cycle, between the base tumble oriented engine and the Swumble™ powered engine. It is also important to mention that the two cases have the same combustion phasing. When running the Swumble™ engine, higher maximal TKE results combined with a better distribution with high values close to the spark plug electrodes is observed. Moreover, the flame front (shown as a black solid line) has a symmetrical evolution, having already covered a larger area of the domain under the exhaust valves, when compared to the tumble base case. This result has an important influence on the improved knock propensity which will be discussed further on.

2.4 Combustion performances

Combustion duration

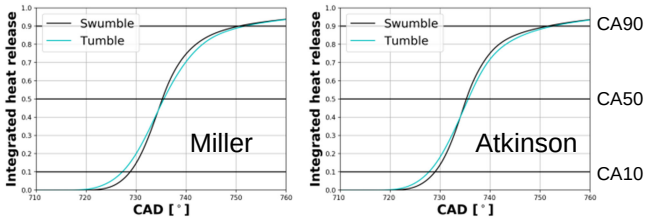

Figure 8. Normalised integrated heat release.

In Figure 8, a comparison of the combustion performances for the Tumble and Swumble™ engines running on Miller and Atkinson cycles is highlighted. On both cycles, the combustion phasing (MFB50) is fixed at 15° for both engines. In these conditions, the Swumble™ engine combustion duration (MFB90-MFB10) decreases by 2.8° and 2.3° when running on the Miller and Atkinson cycles respectively.

Knock propensity

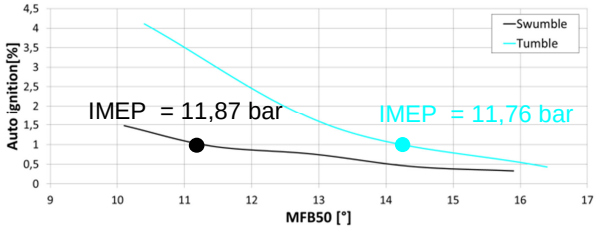

Figure 9. Auto ignition tendency for both Tumble and Swumble™ engines.

$$Auto\ ignition\ [\%] = \frac{m_{ai}[mg]}{m_{pf}[mg]+m_{ai}[mg]} \quad (1)$$

Thanks to the use of the ECFM model for the flame propagation modelling coupled to the TKI model for the auto-ignition modelling, the fuel mass burned in auto-ignition can be distinguished from the fuel mass burnt in conventional flame propagation mode. Equation 1 details the CKI (Computational Knock Index [13]) which is an auto ignition factor representing the ratio between the mass burned by auto ignition (m_{ai}) and the total mass burned during the combustion (sum of the mass burned by flame propagation subsequent to ignition(m_{pf}) and by auto-ignition (m_{ai})). Figure 9 plots the evolution of the auto-ignition factor with respect to the combustion phasing. At iso-IMEP using the Swumble™ concept, a gain of 3 degrees of combustion phasing is obtained.

2.5 Conclusions

The Swumble™ engine allows for better TKE production resulting into lower combustion duration. This allows for higher EGR ratios and better IMEP stability. Referring to knock propensity, the Swumble™ concept allows for reduced knock sensitivity with better combustion phasing.

3 Single cylinder engine

After optimizing the Swumble™ Gen2 design by means of 3D CFD calculations, a single cylinder engine featuring this innovative combustion system was designed and manufactured for performance assessment.

3.1 Engine Configuration

An experimental campaign was performed on the Swumble™ single cylinder 4 valve engine (SCE). The engine presents a 0.400 l displacement, with a centrally mounted multi-hole injector (Bosch HDEV6, 350 bar max injection pressure) and variable valve timing actuation (VVT) for both intake and exhaust. Ignition is provided by a state of the art ignition system featuring a conventional coil and spark plug.

A water cooled pressure sensor (Kistler 6041B) was installed to monitor the combustion process. Engine characteristics are summarized in Table 2.

Variable valve timing regulates the internal gas recirculation rate by adjusting the intake and exhaust valve opening timings, and therefore their overlap. Intake valve spread has a duration of 140°CA (measured at 1 mm valve lift), resulting in an early valve closing, i.e. Miller cycle. As a matter of fact, IFPEN's strategy on Miller / Atkinson cycle is to apply Miller approach on turbocharged applications, and Atkinson approach on naturally aspirated applications, with the objective of optimizing global efficiency. In this work, the final multi-cylinder application is turbocharged.

Injection duration is set to ensure a stoichiometric ratio, regulated by means of an exhaust lambda sensor, and verified through exhaust gas composition analysis. A homogeneous mixture is achieved by setting early injection timing (300 – 330 °CA bTDC).

The engine is equipped with a low pressure EGR circuit, allowing the variation of the EGR rate over a wide range of operating conditions. The temperature of the intake gases (EGR + air) is independently controlled by means of a dedicated heat exchanger.

To mimic the conditions of a turbocharged multi-cylinder engine, intake temperature and exhaust pressure are regulated as a function of the engine speed and mass flow rate by means of a simplified model. The comparison of the simplified model employed in the SCE and the real boundary conditions obtained in the multi-cylinder engine will be discussed in the results section.

To improve the EGR rate control accuracy, exhaust gases are expanded to ambient pressure through a valve, and re-compressed by means of a twin pistons compressor. To avoid damages to the EGR compressors, the gas temperature is decreased down to 20°C and most of the water is separated by condensation. The EGR composition is therefore modified when compared to the multi-cylinder case.

Measurements are taken for the intake and exhaust pressure and temperature, as well as standard exhaust gas analysis of CO, UHC, CH_4, NO_x and smoke. Intake manifold CO_2 analysis helps estimate the EGR rate.

The intake flow rate is also measured to provide, in combination with the exhaust gas analysis, a verification of fuel consumption measurements provided by the fuel balance (AVL733S). Exhaust particle are monitored with an AVL Smoke Meter and with a Horiba MEXA-2000 SPCS particle counting system set to count all the particles down to 10 nm mobility diameter [14].

Finally, the fuel used is a standard E10 with RON 95.

Engine displacement [l]	0.4
Vol. compression ratio [-]	13.45 : 1
Bore x Stroke [mm]	75 x 90.5
Number of intake /exhaust valves	2 / 2
Valve Lift CA duration, at 1mm valve lift [°]	Intake 140 Exhaust 210
Injection system	DI central
Injector	Bosch HDEV6 6 holes
Injection pressure [bar]	350

Table 2. Single cylinder engine main features.

3.2 Operations at Mid-load

Engine parameters were optimized to achieve the best results in ISFC for each working condition by adjusting injection phasing and VVT settings.

Figure 10 and 11 present the results obtained when increasing EGR rates up to the combustion stability limit while keeping all other parameters constant and adjusting combustion phasing to match the knocking – thermodynamic efficiency trade-off. Two mid-load operating conditions are discussed in the section: 3000rpm x 13bar (OC1) and 4000rpm x 16bar (OC2).

At both operating conditions, high EGR dilution can be reached in stable operations (26.4% and 24.8% for OC1 and OC2 respectively).

In agreement with previous observations [12-15-16], EGR dilution is beneficial for engine performances and results in reduction of ISFC and an increase in global efficiency. This effect is mostly due to EGR positive effect on knock control and reduction of heat losses [15,16]. In general, this effect is mitigated by the reduction in combustion speed normally associated with EGR dilution. In the Swumble™ configuration, despite an approximate reduction of 25% in combustion speed at 25% EGR rate (bottom plot of Figure 10), its absolute value is high. As discussed in the previous section, enhanced in-cylinder gas motion provided by the Swumble™ improves turbulences at the TDC with a positive effect on turbulent flame speed and eventually in combustion duration.

Increasing the dilution limit represents a further possibility for increasing the performances of the engine. For both OC1 and OC2, very low instabilities of IMEP are measured up to the dilution limit. The comparison of the measurements to the minimum combustion speed accepted by this kind of engine suggests that combustion speed is not the main factor limiting the EGR dilution. Authors suggest that

the instabilities observed are therefore related to the ignition phase and the early flame propagation. A possible solution to extend the EGR limit could therefore be provided by enhanced ignition systems such as Corona sparks or pre-chambers.

Another important effect of the improved aerodynamics provided by the Swumble™ concept is reflected in an improved homogenization of the gas within the cylinder. This aspect is proved by the low value of pollutant measured (COi and UHCi) and the consequent high value combustion efficiency (Figure 11), despite the very high geometric compression ratio, 13.45 : 1. Also, fuel mixing is of high relevance in GDI engines due to the risk of particulate emissions [17]. The low value of smoke number and PN presented in Figure 11 confirms a good interaction of the fuel spray with the Swumble™ motion.

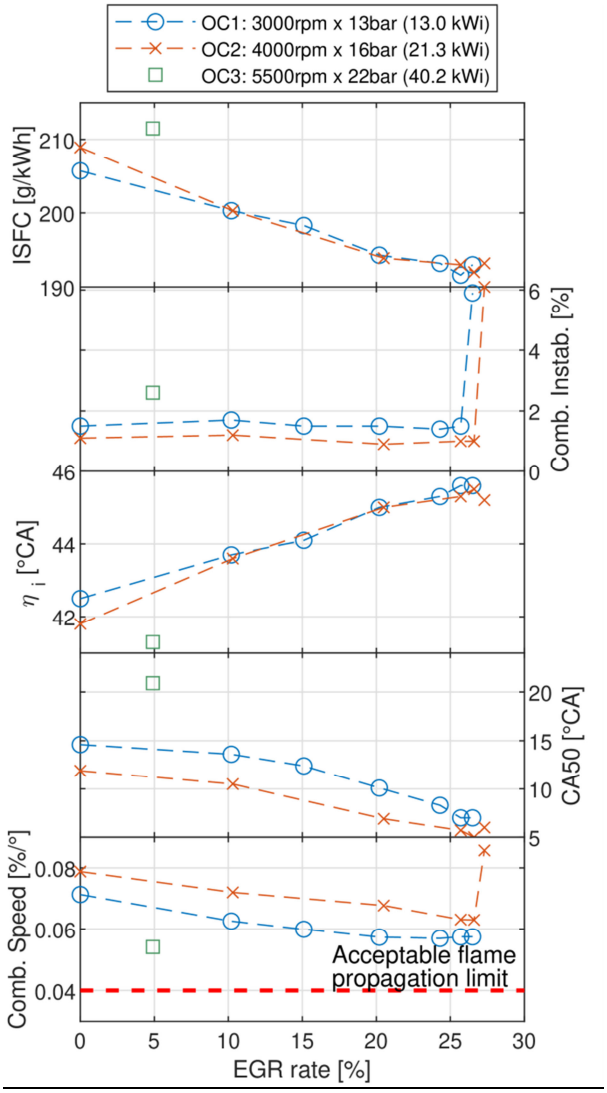

Figure 10. Results from SCE test campaign (part 1/2). Impact of EGR rate on OC 1, 2 and 3 are presented.

3.3 High-load operations and engine map

Figures 10 and 11 also present detailed results of a high-load and high-speed operating condition (OC3 at 5500 rpm for 22 bar IMEP). This condition is of particular interest since it underlines that, despite the high compression ratio and strong Miller approach, this engine configuration enables to reach a remarcable output power (40.2 kWi), corresponding to 100.75 kWi/l power density. It is important to notice that, also at these conditions, the engine tolerates engine dilution (5% EGR). This fact improves knock control and helps reducing engine consumption as indicated by the ISFC measurement (211g/kWhi). As a last remark, this point does not correspond to the engine power output limit, but to what it has been tested up to for the moment. Higher power output might be reached.

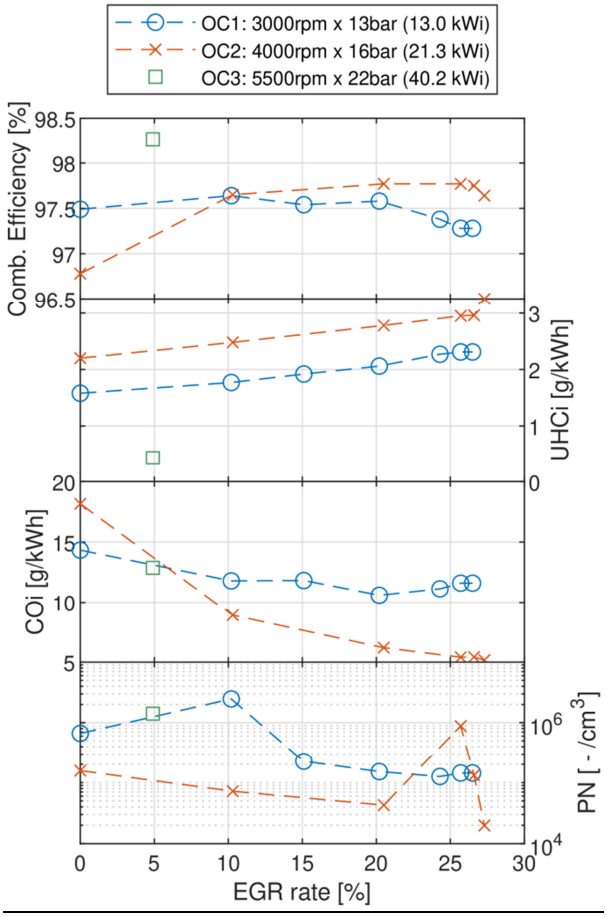

Figure 11. Results from SCE test campaign (part 2/2). Impact of EGR rate on OC 1, 2 and 3 are presented.

Figure 12 presents global results on engine maps. The indicated efficiency map (top part of Figure 12) features a wide core region with values above ηi = 44.5% (corresponding to 196 g/kWhi ISFC) and ηi = 45.5% peak value (191.7 g/kWh). Combustion efficiency results (center map in Figure 12) are relatively flat on the whole engine map proving the

effectiveness of in-cylinder fluid motion on the different parts of the map. This fact is even more important when related to the EGR rate presented in the bottom part of Figure 12. A large portion of the map is operated with EGR rates higher than 25% with a small region above 30%.

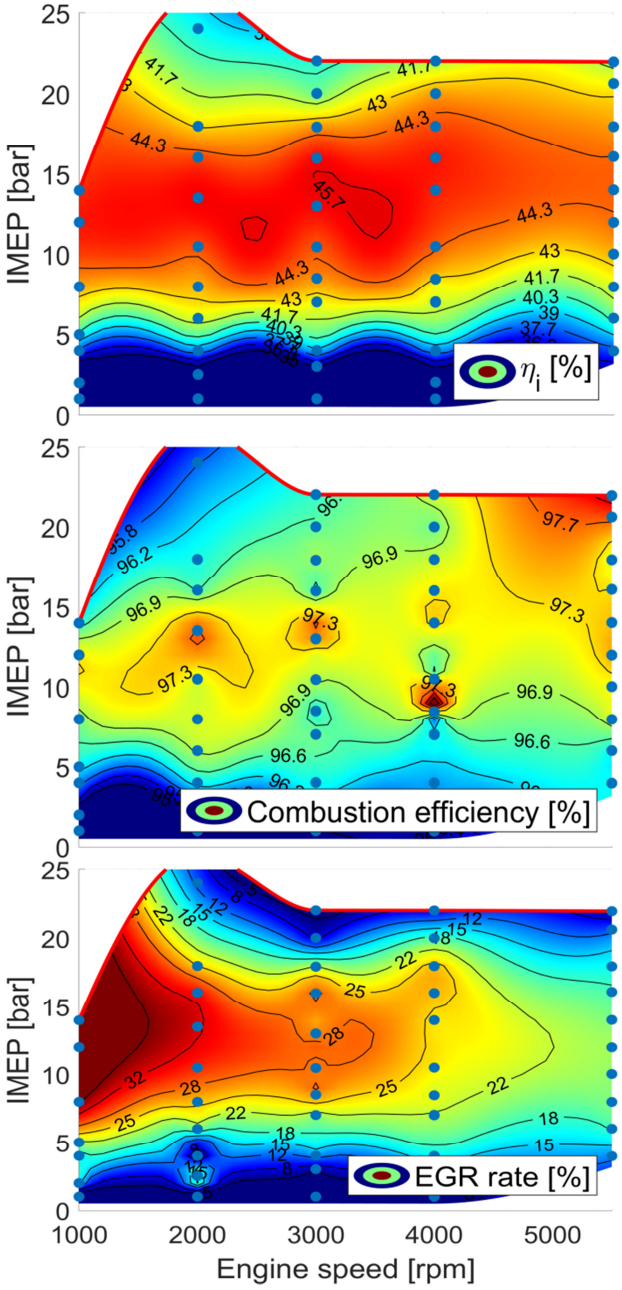

Figure 12. Contours engine maps obtained for SCE. ISFC (top), combustion efficiency (center) and EGR rate (bottom).

In conclusion, the SCE results showed that the Swumble™ approach improves the EGR tolerance of the combustion system while keeping optimal values of combustion efficiency despite the very high compression ratio. This combination of effects results eventually in optimal ISFC levels.

4 Multi-cylinder engine

A three cylinders engine was designed and manufactured with the same combustion system as the single cylinder engine. Engine characteristics are listed in Table 3.

The MCE is based on a *PSA* EB2ADTS 96kW engine on which the serial cylinder head is removed and replaced by IFPEN cylinder head featuring the Swumble™ fluid motion. The cylinder head is equipped, like the SCE, with intake and exhaust Variable Valve Timing systems (VVT), an intake valve spread duration of 140°CA for Miller cycle and a 350 bar injection system to optimize air-fuel mixing and reduce particulate emissions.

Engine displacement [l]	1.2
Vol. compression ratio [-]	13.65 : 1
Bore x Stroke [mm]	75 x 90.5
Number of intake /exhaust valves	2 / 2
Valve lift CA duration, at 1mm [°]	Intake 140 Exhaust 210
Injection system	DI central
Injector	Bosch HDEV6 6 holes
Injection pressure [bar]	350

Table 3. Multi-cylinder engine main features.

4.1 Engine Architecture

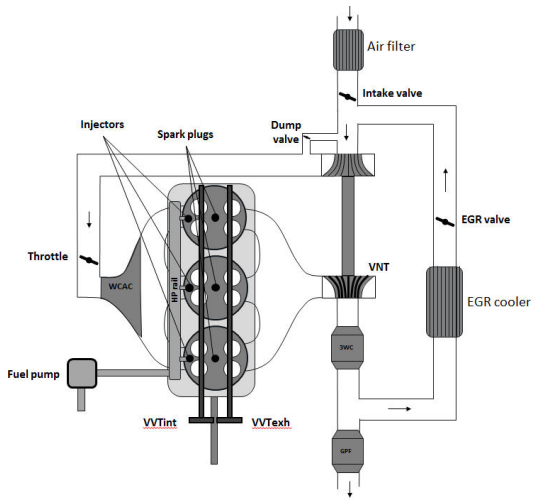

Figure 13. Engine architecture.

The engine has a prototype *Garrett* VNT turbocharger in order to provide the required amount of air at high loads. A *Valeo* prototype water charge air cooler (WCAC) is used in order to cool down the

intake gases coming from the compressor. The WCAC is placed just before the engine intake manifold in order to be as close as possible to the engine. As the gases coming from the compressor may reach high temperatures, a water cooled throttle valve is used.

The VNT turbine is placed just after the engine exhaust, reducing the amount of heat transfer losses. Additionally, there is an exhaust gas recirculation (EGR) system extracting exhaust gases just after the series-production 3-way catalytic converter (3WC). The Gasoline Particulate Filter (GPF) has been removed for this first test phase. The exhaust gases are cooled down by a *Valeo* prototype EGR cooler and reintroduced into the intake system at the compressor inlet. The amount of exhaust gases reintroduced into the system (EGR rate) is regulated via an EGR valve placed just after the EGR cooler. In case the required amount of EGR rate is not achieved by opening completely the EGR valve, an additional valve (intake valve) is placed just before the compressor inlet in order to reduce the pressure and increase the amount of exhaust gases introduced into the intake system.

4.2 Installation

Figure 14 shows the engine test cell. Several pressure and temperature sensors are placed all along the intake and exhaust pipes of the engine. Each cylinder is equipped with Kistler 6041B pressure cylinder sensors. The same apparatus as those used for the SCE were used to perform standard exhaust gas analysis, measurements of soot levels (FSN) and particle number from 10nm.

The engine control is managed by a fully open ECU *McLaren* TAG400i.

Finally, as for SCE experiments, tests are performed using a standard E10 RON 95 gasoline fuel.

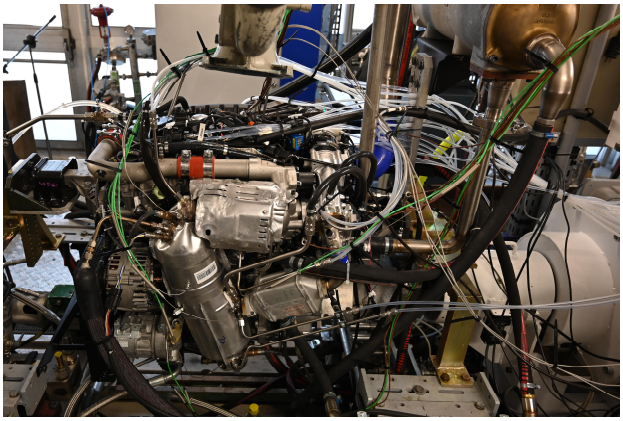

Figure 14: Multi-cylinder engine in test bench

4.3 First results

Oil and water coolant temperature are fixed at 90°C. Inlet air and EGR mixing temperature are regulated by the WCAC in order to respect a plenum temperature map representative of a series-production engine. This temperature map depends on engine speed and intake plenum pressure. Ambient air is regulated around 50% of relative humidity and 20°C at sea level pressure.

Exhaust back pressure just before 3WC is calibrated using the same values than the series-production powertrain with complete after-treatment system (3WC+GPF) and rear muffler.

Figure 15 gives an overview of the first results obtained during the very first weeks of rotation of the engine. For these first optimized operating points, the maximum brake efficiency exceeds 41%. These first results have been obtained considering non optimized FMEP, standard intake temperatures (WCAC not fully operational for those first tests), and with a standard E10 RON 95 gasoline. The combustion efficiency is often above 97% which is a very good value for a high compression engine. Combustion duration (CA90-CA10) is under 22°CA despite EGR rates between 18 and 25%. Particulate emissions are also very low with values below 10^5#/cm^3 on all operating points. These three parameters present good results, which are an indicator of high level of turbulence and good mixture preparation.

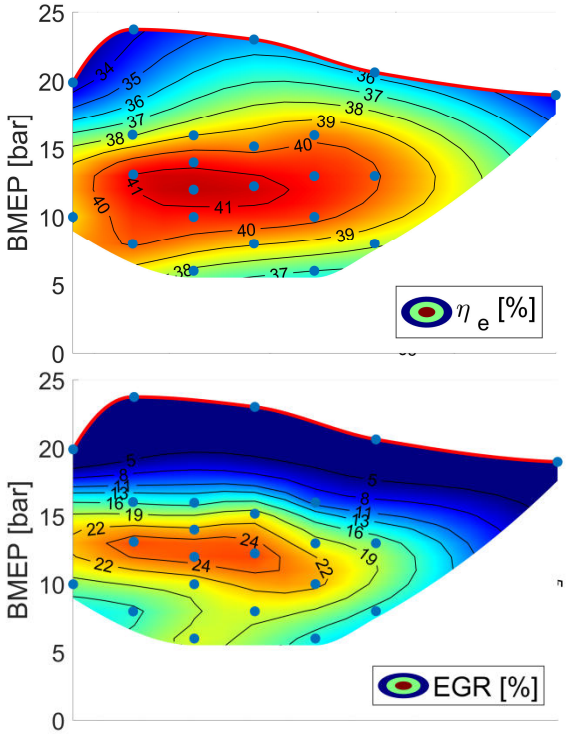

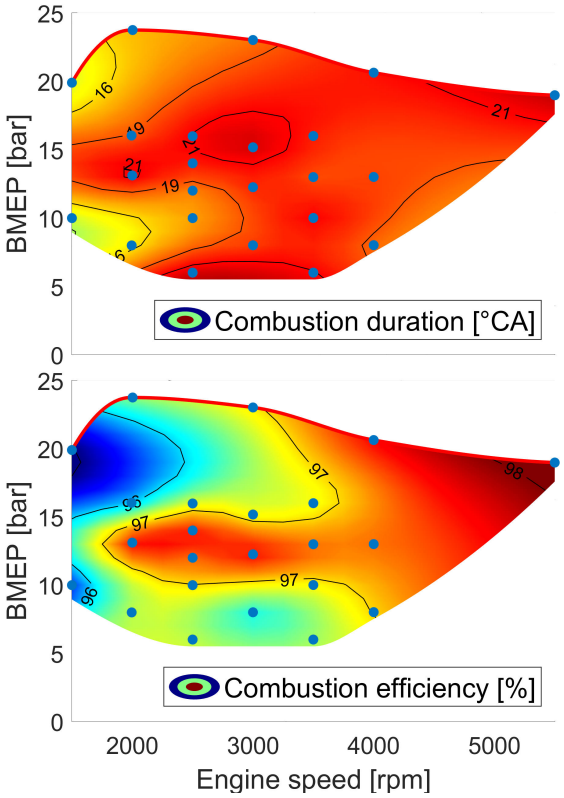

Figure 15. Results from MCE test campaign. Contours engine maps obtained for MCE for the first operating points.

The optimal EGR level is regularly lower on MCE compared to SCE. This is due to the increase of exhaust pressure with the increase of EGR rates. To obtain higher EGR rates, the turbocharger requires more energy to compress the intake mixture and therefore closes the VNT actuator. On the one hand, EGR helps reducing knock and heat wall thermal losses in the combustion chamber. On the other hand, high EGR rates increase pumping losses and should be compensated by the HP-IMEP, i.e. higher combustion loads, which reduces the benefit of EGR because of knock. Figure 16 illustrates this behavior on a 2500 rpm x 14bar BMEP operating point were 25% EGR degrades the optimal ISFC obtained at 22.5% EGR.

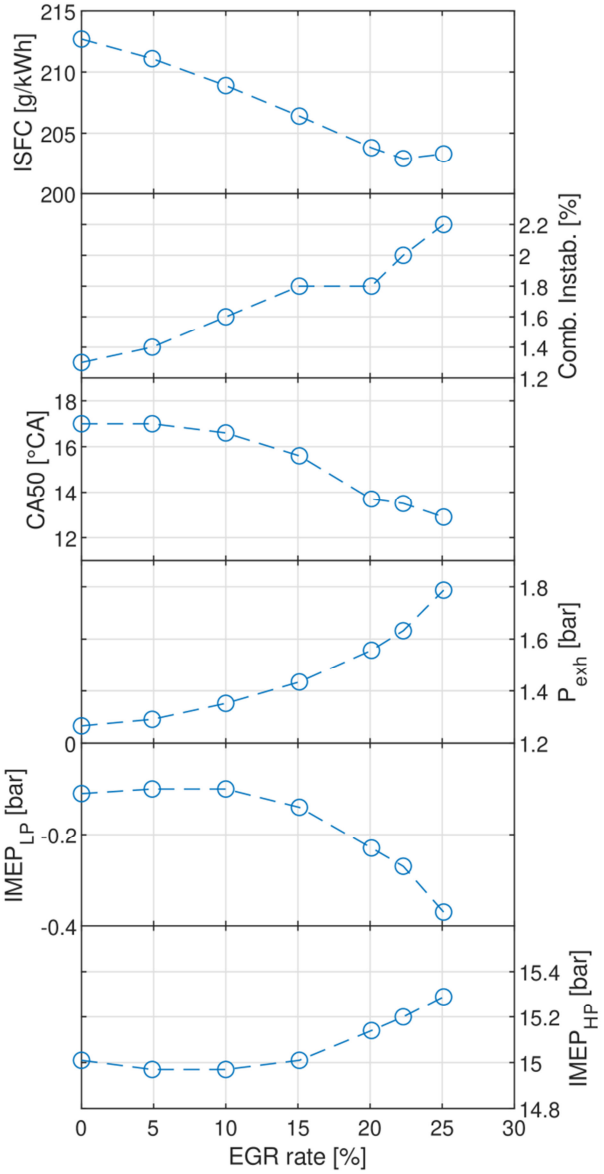

Figure 16. Results from MCE test campaign. Impact of EGR rate at 2500rpm x 14bar BMEP.

This second effect is not visible on SCE with the simplified exhaust pressure model. This mainly explains the 2 points of indicated efficiency difference while comparing MCE and SCE on turbocharged operating points. On a naturally aspirated operating point without EGR, the indicated efficiency is roughly the same. Figure 17 provides a comparison of indicated efficiencies between SCE and MCE at the same IMEP, highlighting the order of magnitude of the differences obtained at different operating conditions.

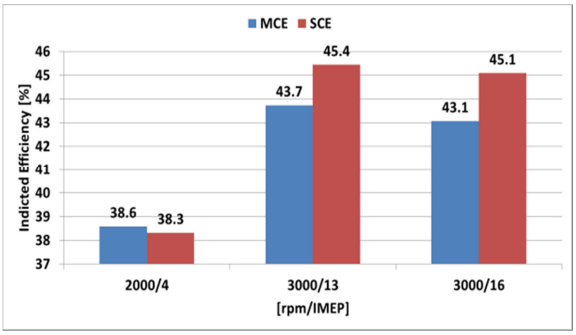

Figure 17. Comparison between SCE and MCE indicated efficiency results at different OC.

Figure 18 details the full load capabilities of the engine. These first results have been obtained considering non optimized water coolant temperature, standard intake temperatures (WCAC not fully operational for these first tests) and with a standard E10 RON 95 gasoline.

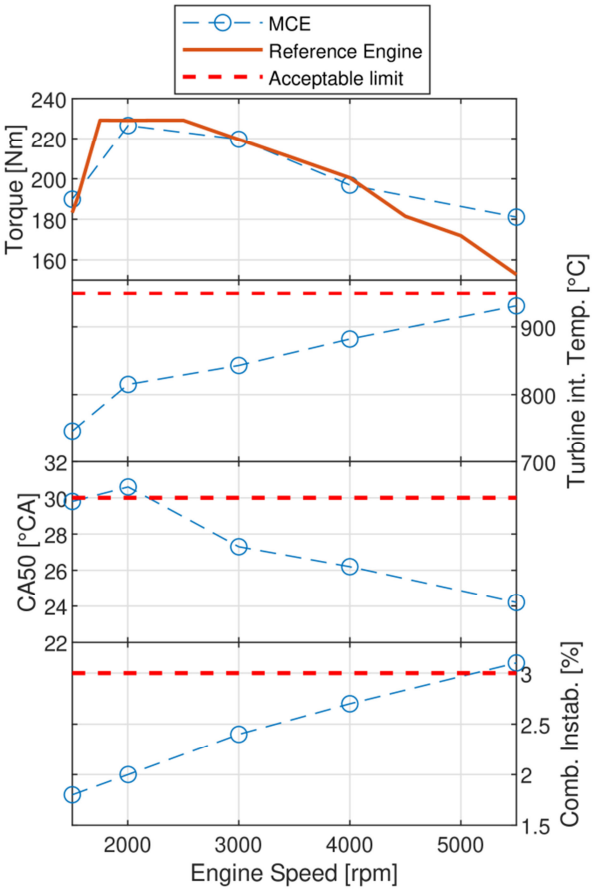

Figure 18. Results from MCE test campaign. Full load curve and comparison with reference data.

Despite the Miller approach employed in this engine (140°CA intake valve duration), the same maximum torque as the reference engine is reached (EB2ADTS), while maintaining lambda 1 values on the entire full load curve. Moreover, the reference maximal output power was improved at 5500 rpm (104 versus 96kW). At low engine rotational speeds, the full load is limited by the maximum CA50 (max 30°CA). At higher engine speeds, the full load is limited by combustion instabilities (max 3%).

5 Conclusion

This paper displays the development path of a new concept for high efficiency spark ignition engines. This concept is based on an innovative fluid motion which combines tumble and swirl creating a Swumble™ motion. No mobile device is used at the intake of the engine to create this Swumble™ motion.

Numerical investigations prove a very good ability to maintain high levels of TKE when using Miller or Atkinson cycle (EIVC or LIVC) on the Swumble™ concept, which a more classical tumble concept dearly lacked. 3D CFD predicts more than 20% improvement in both conditions, thus enabling further gains through more aggressive Miller or Atkinson cycles. Moreover, this new fluid motion does not suffer from higher heat losses or a decrease of flow capacity when compared to the reference engine with a classical tumble motion.

The second step of this development is the optimization on a SCE. The results show that the Swumble™ approach improves the EGR tolerance of the combustion system while keeping optimal values of combustion efficiency, despite the very high compression ratio. This combination of effects results in optimal ISFC levels for a Lambda 1 combustion system: a maximum indicated efficiency close to 46%, combined with a very impressive area higher than 44%, from 9 to 18 bar IMEP, nearly on the whole engine speed range.

Finally, the very first tests on the final multicylinder engine designed embedding the Swumble™ concept confirmed these very promising results. With a 13.65:1 compression ratio and an aggressive Miller cycle, an effective efficiency higher than 41% has already been achieved, together with a very large area higher than 40%. A maximum specific power close to 90 kW/L is obtained, fully lambda one.

This development is still ongoing and several improvement pathways have been identified. These latter are currently being investigated and should provide improved results for future papers and presentations.

6 Acknowledgement

The authors would like to acknowledge:

- Didier Ambrazas, Christophe Lechard, David Bizien and Jérémy Jarry for the design,

manufacturing and assembly of the SCE and MCE

- Luis Enrique Martinez Alvarado for the simulation work to design the MCE EGR loop and provide the SCE air loop model
- Yann Rabois, Adrien Nail for the fine work performed in operating respectively the single cylinder and the multi-cylinder engines.
- Valeo and Garrett for their collaboration on the MCE air loop and the associated hardware provided.

7 Glossary

3WC: 3-way catalytic converter

BMEP: brake mean effective pressure

bTDC: before top dead center

CA: crank angle

ECFM: extended coherent flame model

ECU: electronic control unit

EGR: exhaust gas recirculation

FMEP: friction mean effective pressure

FSN: filter smoke number

GPF: gasoline particles filter

HP IMEP: high pressure indicated mean effective pressure

ISFC: indicated specific fuel consumption

ISSIM: Imposed Stretch Spark Ignition Model

LP IMEP: low pressure indicated mean effective pressure

MCE: multi cylinder engine

MFBXX: crank angle at which XX% of the mass of fuel has burnt

OC: operating conditions

PN: particle number (including particles diameter down to 10nm)

RON: research octane number

SCE: single cylinder engine

TDC: top dead center

TKE: turbulent kinetic energy

VNT: variable nozzle turbine

VVT: variable valve timing

WCAC: water charge air cooler

η_i :indicated global efficiency

η_e : effective global efficiency

8 References

[1] European Commission, “Communication From The Commission To The European Parliament, The European Council, The Council, The European Economic And Social Committee, The Committee Of The Regions And The European Investment Bank". A Clean Planet for all A European strategic long-term vision for a prosperous, modern, competitive and climate neutral economy COM(2018) 773 final, 2018.

[2] European Commission, “Communication From The Commission To The European Parliament, The Council, The European Economic And Social Committee And The Committee Of The Regions". A European Strategy for Low-Emission Mobility,” COM(2016) 501 final, 2016.

[3] International Energy Agency. CO_2 Emissions From Fuel Combustion: Database Documentation; 2018.

[4] Façanha C. Global Transportation Energy and Climate Roadmap; 2012.

[5] Colin O, Truffin K. A spark ignition model for large eddy simulation based on an FSD transport equation (ISSIM-LES). Proceedings of the Combustion Institute 2011;33(2):3097–104.

[6] Colin O, Benkenida A, Angelberger C. 3d Modeling of Mixing, Ignition and Combustion Phenomena in Highly Stratified Gasoline Engines. Oil & Gas Science and Technology - Rev. IFP 2003;58(1):47–62.

[7] Cordier M, Laget O, Duffour F, Gautrot X, Francqueville L de. Increasing Modern Spark Ignition Engine Efficiency: A Comprehension Study of High CR and Atkinson Cycle. In: SAE International400 Commonwealth Drive, Warrendale, PA, United States; 2016.

[8] Guillaume Bourhis, Dr. Olivier Laget, Rajesh Kumar, Xavier Gautrot (ed.). Swumble In-Cylinder Fluid Motion: A Pathway to High Efficiency Gasoline SI Engines; 2018.

[9] Jörg Rückauf, Jürgen Stehlig, Ivano Morgillo, Martin Janssen, Shunichi Inamijima, Masahito Shiraki, Kazuki Tanzawa, Isei Matsuzaki, Junichi Matsuzaki, Takashi Kawano (ed.). Developing a Multistep Tumble Flap for Air Intake Systems; 2017.

[10] Ogink R, Babajimopoulos A. Investigating the Limits of Charge Motion and Combustion Duration in a High-Tumble Spark-Ignited Direct-Injection Engine. SAE International Journal of Engines 2016-01-2245 2016;9(4):2129–41.

[11] Laget O, Zaccardi J-M, Gautrot X, Mansion T, Cotte E. Establishing New Correlations Between In-Cylinder Charge Motion and Combustion Process in Gasoline Engines Through a Numerical DOE. SAE Int. J. Engines 2010;3(1):183–201.

[12] P. Anselmi, X. Gautrot, O. Laget, M. Ritter, C. Lechard (ed.). Swumble In-Cylinder Fluid Motion: a Pathway to High Efficiency Gasoline SI Engines; 2019.

[13] Chevillard S, Colin O, Bohbot J, Wang M,Pomraning E, Senecal PK. Advanced Methodology to Investigate Knock for Downsized Gasoline Direct Injection Engine Using 3D RANS Simulations. In: SAE International400 Commonwealth Drive, Warrendale, PA, United States; 2017.

[14] Horiba Ltd. Horiba Mexa 2000 product specifications. [September 14, 2020]; Available from: https://www.horiba.com/en_en/products/detail/action/show/Product/mexa-2000spcs-series-57/.

[15] Wei H, Zhu T, Shu G, Tan L, Wang Y. Gasoline engine exhaust gas recirculation – A review. Appl. Energy 2012;99:534–44.

[16] Fischer M, Kreutziger P, Sun Y, Kotrba A. Clean EGR for Gasoline Engines – Innovative Approach to Efficiency Improvement and Emissions Reduction Simultaneously. In: SAE International; 2017.

[17] Bardi M, Pilla G, Gautrot X. Experimental assessment of the sources of regulated and unregulated nanoparticles in gasoline direct-injection engines. International Journal of Engine Research 2019;20(1):128–40.